Atmos. Chem. Phys. Discuss., 9, 15725–15746, 2009
www.atmos-chem-phys-discuss.net/9/15725/2009/

Atmospheric Chemistry and Physics Discussions

This discussion paper is/has been under review for the journal *Atmospheric Chemistry and Physics (ACP)*. Please refer to the corresponding final paper in *ACP* if available.

Increasing synoptic scale variability in atmospheric CO_2 at Hateruma Island associated with increasing East Asian emissions

Y. Tohjima[1], H. Mukai[2], S. Hashimoto[2], and P. K. Patra[3]

[1]Atmospheric Environment Division, National Institute for Environmental Studies, Tsukuba, Japan
[2]Center for Global Environmental Research, National Institute for Environmental Studies, Tsukuba, Japan
[3]Research Institute for Global Change, JAMSTEC, Yokohama, Japan

Received: 9 July 2009 – Accepted: 15 July 2009 – Published: 24 July 2009

Correspondence to: Y. Tohjima (tohjima@nies.go.jp)

Published by Copernicus Publications on behalf of the European Geosciences Union.

Abstract

In-situ observations of atmospheric CO_2 and CH_4 at Hateruma Island, Japan show large synoptic scale variations during a 6-month period from November to April, when the sampled air is predominantly of continental origin due to the Asian winter monsoon. Synoptic scale variations are extracted from the daily averaged values for the years between 1996 and 2007, along with the annual standard deviations (σ_{CO_2} and σ_{CH_4} for CO_2 and CH_4, respectively) for the relevant 6-month period. The temporal change in σ_{CO_2} shows a systematically increasing trend over the 12-year period, with elevated excursions in 1998 and 2003; there is no clear trend in σ_{CH_4}. We also find that the $\sigma_{CO_2}/\sigma_{CH_4}$ ratio increases gradually from 1996 to 2002 and rapidly thereafter 2002 without any extreme deviations that characterized σ_{CO_2}. The $\sigma_{CO_2}/\sigma_{CH_4}$ ratio correlates closely with the recent rapid increase in fossil carbon emission from China, as indicated in the CDIAC data. This methodology can be applied for tracking overall changes in regional emissions by measuring multiple chemical tracers.

1 Introduction

Increase in carbon dioxide (CO_2) emission from fossil fuel consumption, cement manufacturing, and decomposition of biomass and soil organic matter associated with land-use changes has contributed to the observed rise in atmospheric CO_2 since the industrial revolution. Although on average, more than half of the anthropogenic CO_2 has been taken up by the land biosphere and the ocean, the recent growth rate of atmospheric CO_2 shows a gradual increasing trend mainly due to the continuous increase in fossil fuel consumption (e.g. Keeling et al., 1995; Patra et al., 2005). Although there are international efforts to reduce the greenhouse gas emissions, the global CO_2 emission from fossil fuel consumption and cement manufacturing derived from the Carbon Dioxide Information Analysis Center (CDIAC) database (Marland et al., 2007) shows an unprecedented accelerated growth during the period of 2002–2005. This rapid

ACPD

9, 15725–15746, 2009

emission growth has been attributed to the accelerating emissions from the developing countries (Raupach et al., 2007), especially China (Gregg et al., 2008).

Increasing fossil fuel CO_2 emissions elevate not only the overall global atmospheric burden but also enhance the local atmospheric concentrations relative to the surrounding regions. Thus, a greater emission intensity will produce larger concentration gradient in the downwind region, resulting in a greater synoptic scale variation (SSV) in the CO_2 concentration when synoptic winds change directions. For example, the Chinese CO_2 emission data from the CDIAC database indicate a rapid increase from 0.9 Pg C in 2000 to 1.5 Pg C in 2005, which could affect the SSVs in the East Asian regions. Since the amplitude of SSVs will likely change as a function of the source-receptor distance and the source strength, a SSV ratio of two chemical tracers (such as CO_2 and CH_4 employed in this study) with a similar emission pattern and long lifetime (~month–year) would conserve the ratio of the source strengths robustly.

The National Institute for Environmental Studies (NIES) has been carrying out in-situ measurements of atmospheric greenhouse gases, including CO_2 and methane (CH_4), at Hateruma Island (HAT, 24.05° N, 123.80° E), which is located in the East Asian continental margin. The observations at HAT often show pollution events influenced by the continental emissions during the period from the late fall to early spring each year (Tohjima et al., 2000, 2002; Yokouchi et al., 2006). Recently, analyses of the SSVs have been found to be useful for validating regional fluxes with the help of a chemical transport model (Patra et al., 2009). In this paper, we examine the temporal changes in atmospheric CO_2 SSVs observed at HAT during 1996–2007 and investigate its relationship with the continental fossil CO_2 emissions. The CO_2 SSVs are usually associated with similar SSVs in CH_4 observed at HAT. Therefore, the ratio of CO_2 and CH_4 SSVs is used to construct a conservative tracer for tracking emission changes over the source regions.

ACPD
9, 15725–15746, 2009

2 Data and methods

We use daily averages of the atmospheric CO_2 and CH_4 concentrations observed at HAT. The CO_2 concentrations were continuously measured by a nondispersive infrared analyzer (NDIR) (Mukai et al., 2001) and the CH_4 concentrations were semi-continuously measured by a gas chromatography equipped with an FID (Tohjima et al., 2002). To characterize the air mass transport to HAT, we calculate kinematic 3-day backward trajectories with arrival time of 0600 UTC (1500 JST) and starting altitude of 500 m a.s.l. by using the METEX (METeorological data EXplorer, http://db.cger.nies.go.jp/metex/) program developed by Zeng et al. (2003).

The observed CO_2 and CH_4 variations include not only SSVs but also long-term trends, regular and irregular seasonal variations. Thus, we first obtain smooth-curve fits to the data following the methods of Thoning et al. (1989) with a cut-off frequency of 4.6 cylces yr^{-1}, roughly corresponding to a 40-day running average. Then we subtract the smooth-curve fits from the original time series to extract the SSV components, which are denoted by the Δ notation as ΔCO_2 and ΔCH_4 (similar to that used in Patra et al., 2008). Figure 1 depicts the time series of ΔCO_2 and ΔCH_4 in 2000 as a typical example. It should be noted that these time series show noticeably similar variations each other during the periods from January to April and from November to December. Annual standard deviations of ΔCO_2 and ΔCH_4 (defined as σ_{CO_2} and σ_{CH_4}) are calculated using the data from January to April and from November to December. The data for the period May to October are not used in this study. We also investigate the ratio of σ_{CO_2} to σ_{CH_4}. Note that the daily data are applied to these analyses only when both CO_2 and CH_4 data exist.

We extend the analysis of the observed SSVs by simulating the daily averages of CO_2 and CH_4 at HAT with a chemistry-transport model (ACTM) possessing a horizontal resolution of T42 spectral truncation (~2.8°×2.8°) and 67 sigma-pressure vertical layers. The transport model is driven by an atmospheric general circulation model (AGCM). The capability of the ACTM to simulation CO_2 and CH_4 has been investi-

ACPD
9, 15725–15746, 2009

gated elsewhere (Patra et al., 2008, 2009). We use the CH_4 emission scenario (E2 scenario) developed in Patra et al. (2009) that optimally fits the interhemispheric gradient and seasonal cycles at most sites around the globe to within about 10 ppb on an average. For the CO_2 simulation, annually balanced terrestrial ecosystem flux (Randerson et al., 1997), oceanic exchange (Takahashi et al., 2008) and fossil fuel emission (Olivier and Berdowski, 2001) are used in simultaneously. While the monthly-mean terrestrial and oceanic fluxes are repeated every year, the annual-mean fossil flux is increased/decreased year-to-year as dictated by the CDIAC trends database for individual countries (Marland et al., 2007).

3 Results

The backward trajectories of the air masses arriving at HAT in 2000 during the 6-month period (January–April and November–December) are depicted in Fig. 2. During this period, observations at HAT are dominantly influenced by the air masses transported from the East Asian continental regions. On the other hand, the maritime air masses over the Pacific Ocean are dominantly transported to the site during the period from May to October (trajectories not shown). Such clear transport patterns are caused by the East Asian winter monsoon, and are climatologically characteristic of this region. Because the November–April period is biologically dormant, limiting our analysis to this period has an advantage of reduced, if not negligible, influence from interannual variations in the land biosphere-atmosphere CO_2 exchange. A more detailed investigation of the backward trajectories shows that the observation at HAT is affected by the emissions from the provinces around Beijing (21%), along the east coast of China around Shanghai (17%), Korea (12%), and southern part of Japan (12%). The leading edge of the CO_2 SSV peak is produced mostly when the air mass is directly transported from the source regions, while the trailing edge is associated with the air mass that travels longer over the ocean, circling clockwise around the site. Similar conditions characterize the atmospheric CH_4 SSV peaks throughout the year since CH_4 has

ACPD
9, 15725–15746, 2009

similar emission pattern.

The temporal changes in σ_{CO_2} and σ_{CH_4} are shown in Fig. 3. There are large interannual variations in both σ timeseries; especially the simultaneous abrupt enhancements in 1998 and 2003 are noteworthy. However, if we exclude the anomalously high σ_{CO_2} values in 1998 and 2003, the temporal change shows an apparent secular increase over the whole period, that is, a gradual increase during 1996–2002 and a sharp rise during 2002–2007, resembling the growth rate of estimated annual-total fossil CO_2 emission from China (see Fig. 4). On the other hand, the temporal changes in σ_{CH_4} do not show a clear increasing or decreasing trend, even after the anomalous σ_{CH_4} in 1998 and 2003 are removed.

Figure 4 shows a time variation in the $\sigma_{CO_2}/\sigma_{CH_4}$ ratio as a robust estimation of relative change in emissions. For instance, slower or faster transport from the source region to the measurement site will decrease or increase the SSV peak magnitudes, respectively. By normalizing σ_{CO_2} with respect to σ_{CH_4} such transport effect due to climate variations would be eliminated. However, disproportional changes in the emission ratio of CO_2 and CH_4 would still show up, likely contributing to the differences in the SSV increase for CH_4 and CO_2 in 1998 and 2003, or the appearance of interannual variations in the $\sigma_{CO_2}/\sigma_{CH_4}$ ratio time series (given the fact that the emission distribution of the two species are not exactly the same). The interannual variability in the ratio is substantially reduced in comparison with σ_{CO_2}, and the ratio clearly shows a steadily increasing trend. For comparison, annual time series of national carbon emissions from fossil fuel combustion and cement production for China, Japan, and Korea taken from the CDIAC database (1996–2005) and the US Department of Energy Energy Information Administration (EIA, http://www.eia.doe.gov) database (1996–2006) are also plotted in Fig. 4. Note that the carbon emissions from cement production in the CDIAC dataset are added to the EIA dataset and that the emissions from Japan and Korea shown in Fig. 4 are multiplied by a factor of 5. The national emissions from CDIAC and EIA agree with each other to within ~7% for China, ~5% for Japan, and ~15% for Korea. There is a good agreement between the temporal changes in the $\sigma_{CO_2}/\sigma_{CH_4}$

ACPD
9, 15725–15746, 2009

ratio and fossil carbon emission from China: both temporal changes show a gradual increase during 1996–2002 and a rapid increase during 2002–2005, especially in 2004. While the EIA dataset for China still shows growing emissions in 2006, the observed $\sigma_{CO_2}/\sigma_{CH_4}$ ratio shows a considerable decrease in 2006.

The time series of σ_{CO_2} and σ_{CH_4} and the $\sigma_{CO_2}/\sigma_{CH_4}$ ratio based on the simulated CO_2 and CH_4 are also depicted in Figs. 3 and 4, respectively, as open symbols with broken lines. The temporal changes in σ_{CO_2} and σ_{CH_4} produced by the model simulation also show anomalies in 1998 and 2003, although the amplitudes of the both CO_2 and CH_4 variations are smaller in 2003 in comparison with the observation. The temporal changes in the $\sigma_{CO_2}/\sigma_{CH_4}$ ratio show a better correspondence between the model simulation and the observation than those for σ_{CO_2} and σ_{CH_4}. This result suggests the effectiveness of the normalization of σ_{CO_2} with respect to σ_{CH_4} to reduce the transport effect.

Squared Pearson correlation coefficients (r^2) of the observed $\sigma_{CO_2}/\sigma_{CH_4}$ ratio and the σ_{CO_2} values with the reported fossil carbon emissions from China, Japan and Korea are summarized in Table 1. Most of the correlations are statistically significant. As for the $\sigma_{CO_2}/\sigma_{CH_4}$ ratio, the emission from China for 1996–2005 based on both the CDIAC and EIA data accounts for the highest portion of the temporal variation. However, when the emission for 2006 is included in the EIA data, correlation coefficients between the $\sigma_{CO_2}/\sigma_{CH_4}$ ratio and the emission from China is slightly reduced because of the sudden decrease in the $\sigma_{CO_2}/\sigma_{CH_4}$ ratio and the continued increase in the emission in 2006. On the other hand, although the temporal changes in the σ_{CO_2} values also show the highest correlation with the emission from China, the correlation coefficient is much lower than those for the $\sigma_{CO_2}/\sigma_{CH_4}$ ratio. However, if the anomalous values of 1998 and 2003 are removed, the correlation between the σ_{CO_2} values and the emission from China increases to 0.92 even if the σ_{CO_2} value in 2006 is included. Furthermore, the national emission ratio of CO_2 to CH_4 for China, based on the November–April monthly fluxes used in the model simulation, is almost identical to, but those for Japan and Korea are more than double, the $\sigma_{CO_2}/\sigma_{CH_4}$ ratio at HAT. Moreover, the relative change

ACPD
9, 15725–15746, 2009

in the national emission ratio (CO_2/CH_4) for China against the $\sigma_{CO_2}/\sigma_{CH_4}$ ratio is almost constant (~1) during 1996–2005, while those for Japan and Korea show a gradual decrease (Fig. 5). These results strongly suggest that the SSVs at HAT are affected predominantly by the emissions from China.

4 Discussion

The years of 1997/1998 and 2002/2003 correspond to strong and moderate El Nino periods, respectively. El Nino events alter wind and radiation (outgoing long-wave readiation (OLR), for example) patterns (Fig. 6), causing anomalous transport and anomalous enhancement of CO_2 and CH_4 concentrations in the source region that could explain the enhanced variability in CO_2 and CH_4 at HAT observed in 1998 and 2003. Indeed, a relatively good qualitative agreement between the ACTM simulated and observed variations in σ_{CH_4} at HAT (Fig. 3) is indicative of the significant role the interannual transport variation plays in causing the observed interannual synoptic-scale variation, since nearly constant CH_4 emissions are used in the model, as well as the neglect of the interannual variation in OH (Patra et al., 2009). The $\sigma_{CO_2}/\sigma_{CH_4}$ ratio reduces this transport effect, as noted earlier. We also contend that, within the confines of our study, any change in the $\sigma_{CO_2}/\sigma_{CH_4}$ ratio is mostly reflective of a change in the fossil fuel CO_2 emission. Although interannual climate variations in such parameters as land temperature and precipitation, or in biomass burning can lead to disproportionate release/uptake of CO_2 and CH_4 due to differences in the emission factors associated with different land surfaces (e.g., wetland area, agricultural land), ecosystem types (e.g., grassland, savannah, tree), and processes involved (Andreae and Merlet, 2001), we will argue below that these have minimal effects on our results.

Past El Nino events have certainly influenced the global sources of CH_4 and CO_2 in various ways. For example, unusually large boreal forest fires in eastern Russia from May to October in 1998 and 2002/2003 (Kasischke et al., 2005) would have contributed to the enhancement of σ_{CO_2} and σ_{CH_4}, but since these events occurred outside of the 6-

ACPD
9, 15725–15746, 2009

month period under study, the impact of the biomass burning on our study result regarding the $\sigma_{CO_2}/\sigma_{CH_4}$ ratio is minimal. Similarly, the CH_4 emissions from seasonal sources including wetlands and rice fields in East Asia during the analysis period (November–April) are much smaller than the emissions from the year-round non-seasonal sources including livestock, energy use (coal and natural gas) and landfills. For example, CH_4 emission from Chinese rice fields occurs from April to November, with maximum emission observed in August and more than 70% of the total CH_4 is emitted between June and August (Yan et al., 2003). In addition, the growth rate of the global atmospheric CH_4 burden showed a rapid decreasing trend after 1980, reaching ±5 ppb/yr during 1996–2005 (with the exception of 1998) (Simpson et al., 2006), unlike the rapidly increasing CO_2 from fossil fuel sources. A forward model simulation shows that a nearly constant global CH_4 emission during 1995–2006 is able to reproduce the observed atmospheric CH_4 change with a fixed OH distribution (Patra et al., 2009), supporting the recent stable CH_4 source strength. Anthropogenic CH_4 emission estimates from REAS 1.11 (Regional Emission inventory in ASia) also show that the variability in the estimated yearly anthropogenic CH_4 emission from China is less than ±3%. Furthermore, there is little contribution of the photosynthetic uptake to the CO_2 emission from East Asian continent during the yearly 6-month period under study; heterotrophic respiration is also relatively small during the colder 6-month period compared to the rest of the year (Ito, 2008). It is our contention that the above discussion lend sufficient support to our assumption that the observed $\sigma_{CO_2}/\sigma_{CH_4}$ ratio for the seasonal period of November to April at HAT is predominantly reflective of the changes in fossil CO_2 emissions in East Asia.

To investigate the influence of the regional CO_2 emission variation to the SSVs at HAT, we categorize the origins of the air masses arriving at HAT into 4 regions (China (CH), Japan and Korea (JK), the subtropics (ST), and the Pacific Ocean (PO)) by using the 3-day backward trajectories. We designate the trajectory as CH, JK, and ST when the backward pathway first across the corresponding regional boundaries. The remaining trajectories are designated as PO. In this study the regional boundaries for CH and

ACPD
9, 15725–15746, 2009

JK are the borders of the corresponding countries with resolution of 1°×1° degree, and for ST the border of Taiwan and latitude of 20° N. The results of the categorization of the backward trajectories for 2000 are also illustrated by different colors in Fig. 2. The percentages of the trajectories occurring in these categorized origins are about 38%, 24%, 9%, and 29% for CH, JK, ST, and PO, respectively.

Temporal variation in σ_{CO_2} associated with each of the geographical categories is plotted in Fig. 7, together with that derived from all ΔCO_2. The changes observed in σ_{CO_2} for CH and PO show an increasing trend that is similar to the overall trend. The large variability in σ_{CO_2} for ST is attributed to occasional transport of highly polluted air. On the other hand, the σ_{CO_2} time series for JK shows nearly no trend during the entire 12-year period. These results are consistent with the trend of the recent fossil CO_2 emission from China, Japan, and Korea, suggesting that the air masses originated from JK region do not significantly contribute to the increase in the SSVs in CO_2 at HAT. The increasing trend in PO σ_{CO_2} is likely due to the transport of maritime air mass contaminated by continental air from China.

The footprint of the backward trajectories reaching HAT effectively covers the CO_2 emission centers in China, including the provinces around Beijing and along the east coast of China (Gregg et al., 2008). This may be the reason why the $\sigma_{CO_2}/\sigma_{CH_4}$ ratio at HAT appears to closely track the pattern of the CO_2 emission trend from China during the period from 1996 to 2005, as indicated in the recently revised version of the CDIAC data used in this study (Marland et al., 2007). In the previous version of the CDIAC data, the emission from China decreased by about 20% during 1996–2000, which was mainly based on the official Chinese statistics reporting substantial reduction in fuel consumption, coal consumption in particular, during the aforementioned period. Several researchers questioned the official statistics based on the investigations of various energy statistics and the satellite observations of NO_x over China (Akimoto et al., 2006; Zhang et al., 2007). The gradual increase during 1996–2002 and the rapid increase thereafter in the $\sigma_{CO_2}/\sigma_{CH_4}$ ratio at HAT support the recently revised Chinese emission reflected in the CDIAC data.

ACPD
9, 15725–15746, 2009

The values of the $\sigma_{CO_2}/\sigma_{CH_4}$ ratio at HAT in 2006 and 2007 are considerably lower than and similar to the ratio observed in 2005, respectively. These temporal changes seem to suggest that the increasing rate of fossil CO_2 from China slowed down. However, plotting the values of the $\sigma_{CO_2}/\sigma_{CH_4}$ ratio, excluding those associated with air masses originating from JK and ST, as shown in Fig. 4, we find that the $\sigma_{CO_2}/\sigma_{CH_4}$ ratio for 2007 is higher than that for 2005 although the dip in 2006 is still present. We believe that the selected $\sigma_{CO_2}/\sigma_{CH_4}$ ratio values better reflect the emissions from China than the unselected ratio values. In addition, since σ_{CO_2} shows the highest value in 2007 (Fig. 3), it likely that the increasing trend of the fossil CO_2 emission from China continued through 2007 although the sharp dip in the $\sigma_{CO_2}/\sigma_{CH_4}$ ratio in 2006 still difficult to explain at this time.

Our simple study presented in this paper has shown that the synoptic scale variations in CO_2 and CH_4 observed at HAT can be used to obtain a better estimate of changes in emission from East Asia, especially China. This is important because there is still more than 15% uncertainty associated with the present estimate of the fossil CO_2 emission from China (Gregg et al., 2008). Recently, Stohl et al. (2009) have developed a new inversion method based on a Lagrangian particle dispersion model to estimate regional and global emissions and applied to in-situ measurements of halocarbons from several globally distributed sites. They have found that the emission from China is well constrained by the measurements at HAT. In a similar vein, such inversion method could be applied to our CO_2 data to obtain quantitative fossil CO_2 emission estimation for China during the Asian winter monsoon seasons.

Acknowledgements. We gratefully acknowledge Nobukazu Oda and other staff members of the Global Environment Forum and the staff of Center for Global Environmental Research for their continued support in maintaining the in-situ measurements of CO_2 and CH_4 at HAT. We also thank Toshinobu Machida, Tomonori Watai, and Keiichi Katsumata for determining CO_2 and CH_4 concentrations of the reference gases used at HAT. We wish to thank Jiye Zeng for calculating backward trajectories. This work was partly supported by the Grants-in-Aid for Creative Scientific Research (2005/17GS0203) of the Ministry of Education, Science, Sports and Culture, Japan.

References

Akimoto, H., Ohara, T., Kurokawa, J., and Horii, N.: Verification of energy consumption in China during 1996–2003 by using satellite observational data, Atmos. Environ., 40, 7663–7667, 2006.

Andreae, M. O. and Merlet, P.: Emission of trace gases and aerosols from biomass burning, Global Biogeochem. Cy., 15, 955–966, 2001.

Gregg, J. S., Andres, R. J., and Marland, G.: China: Emissions pattern of the world leader in CO_2 emissions from fossil fuel consumption and cement production, Geophys. Res. Lett., 35, L08806, doi:10.1029/2007GL032887, 2008.

Ito, A.: The regional carbon budget of East Asia simulated with a terrestrial ecosystem model and validated using AsiaFlux data, Agric. For. Meteorol., 148, 738–747, doi:10.1016/j.agrformet.2007.12.007, 2008.

Kasischke, E. S., Hyer, E. J., Novelli, P. C., Bruhwiler, L. P., French, N. H. F., Sukhinin, A. I., Hewson, J. H., and Stocks, B. J.: Influences of boreal fire emissions on Northern Hemisphere atmospheric carbon and carbon monoxide, Global Biogeochem. Cycles, 19, GB1012, doi:10.1029/2004GB002300, 2005.

Keeling, C. D., Whorf, T. P., Wahlen, M., and van der Plicht, J.: Interannual extremes in the rate of rise of atmospheric carbon dioxide since 1980, Nature, 375, 666–670, 1995.

Marland, G., Boden, T. A., and Andres, R. J.: Global, regional, and national CO_2 emissions, Carbon Dioxide Inf. Anal. Cent., Oak Ridge Natl. Lab., US Dep. Of Energy, Oak Ridge, Tenn. (http://cdiac.ornl.gov/trends/emis/tre_regn.html), 2007.

Mukai, H., Katsumoto, M., Ide, R., Machida, T., Fujinuma, Y., Nojiri, Y., Inagaki, M., Oda, N., and Watai, T.: Characterization of atmospheric CO_2 observed at two-background air monitoring stations (Hateruma and Ochi-ishi) in Japan (abstract), paper presented at Sixth International Carbon Dioxide Conference, Organ. Comm. of Sixth Int. Carbon Dioxide Conf., Sendai, Japan, 2001.

Olivier, J. G. J. and Berdowski, J. J. M.: Global emissions sources and sinks, in: The Climate system, edited by: Berdowski, J., Guicherit, R., and Heij, B. J., A. A. Balkema Publishers/Swets & Zeitlinger Publishers, Lisse, The Netherlands, ISBN 9058092550, 33–78, 2001.

Patra, P. K., Maksyutov, S., and Nakazawa, T.: Analysis of atmospheric CO_2 growth rates at Mauna Loa using CO_2 fluxes from an inverse model, Tellus, 57B, 357–365, 2005.

ACPD

9, 15725–15746, 2009

Patra, P. K., Low, R. M., Peters, W., Rödenbeck, C., Takigawa, M., Aulagnier, C., Baker, I., Bergmann, D. J., Bousquet, P., Brandt, J., Bruhwiler, L., Cameron-Smith, P. J., Christensen, J. H., Delage, F., Denning, A. S., Fan, S., Geels, C., Houweling, S., Imasu, R., Karstens, U., Kawa, S. R., Kleist, J., Krol, M. C., Lin, S.-J., Lokupitiya, R., Maki, T., Maksyutov, S., Niwa, Y., Onishi, R., Parazoo, N., Pieterse, G., Rivier, L., Satoh, M., Serrar, S., Taguchi, S., Vautard, R., Vermeulen, A. T., and Zhu, Z.: TransCom model simulations of hourly atmospheric CO_2: Analysis of synoptic-scale variations for the period 2002–2003, Global Biogeochem. Cycles, 22, GB4013, doi:10.1029/2007GB003081, 2008.

Patra, P. K., Takigawa M., Ishijima, K., Choi, B.-C., Cunnold, D., Dlugokencky, E. J., Fraser, P., Gomez-Pelaez, A. J., Goo, T.-Y., Kim, J.-S., Krummel, P., Langenfelds, R., Meinhardt, F., Mukai, H., O'Doherty, S., Prinn, R. G., Simmonds, P., Steele, P., Tohjima. Y., Tsuboi, K., Uhse, K., Weiss, R., Worthy, D., and Nakazawa, T.: Growth rate, seasonal, synoptic, diurnal variations and budget in lower atmospheric methane, J. Meteorol. Soc. Japan, in press, 2009.

Randerson, J. T., Thompson, M. V., Conway, T. J., Fung, I. Y., and Field, C. B.: The contribution of terrestrial sources and sinks to trends in the seasonal cycle of atmospheric carbon dioxide, Global Biogeochem. Cy., 11(4), 535–560, 1997.

Raupach, M., Marland, G., Ciais, P., Le Quere, C., Canadell, J. G., Klepper, G., and Field, C.: Global and regional drivers of accelerating CO_2 emissions, Proc. Natl. Acad. Sci. USA, 104, 10288–10293, 2007.

Simpson, I. J., Rowland, F. S., Meinardi, S., and Blake, D. R.: Influence of biomass burning recent fluctuations in the slow growth of global tropospheric methane, Geophys. Res. Lett., 33, L22808, doi:10.1029/2006GL027330, 2006.

Stohl, A., Seibert, P., Arduini, J., Eckhardt, S., Fraser, P., Greally, B. R., Lunder, C., Maione, M., Mühle, J., O'Doherty, S., Prinn, R. G., Reimann, S., Saito, T., Schmidbauer, N., Simmonds, P. G., Vollmer, M. K., Weiss, R. F., and Yokouchi, Y.: An analytical inversion method for determining regional and global emissions of greenhouse gases: Sensitivity studies and application to halocarbons, Atmos. Chem. Phys., 9, 1597–1620, 2009, http://www.atmos-chem-phys.net/9/1597/2009/.

Takahashi, T., Sutherland, S. C., Wanninkhof, R., Sweeney, C., Feely, R. A., Chipman, D. W., Hales, B., Friederich, G., Chavez, F., Sabine, C., Watson, A., Bakker, D. C. E., Schuster, U., Metzl, N., Yoshikawa-Inoue, H., Ishii, M., Midorikawa, T., Nojiri, Y., Körtzinger, A., Steinhoff, T., Hoppema, M., Olafsson, J., Arnarson, T. S., Tilbrook, B., Johannessen, T., Olsen, A.,

ACPD

9, 15725–15746, 2009

Bellerby, R., Wong, C. S., Delille, B., Bates, N. R., and de Baar, H. J. W.: Climatological mean and decadal change in surface ocean pCO_2, and net sea-air CO_2 flux over the global oceans, Deep-Sea Res. II, 56, 554–577, doi:10.1016/j.dsr2.2008.12.009, 2009.

Thoning, K.W., Tans, P. P., and Komhyr, W. D.: Atmospheric carbon dioxide at Mauna Loa Observatory 2. Analysis of the NOAA GMCC data, 1974–1985, J. Geophys. Res. 94, 8549–8565, 1989.

Tohjima, Y., Mukai, H., Maksyutov, S., Tkahashi, Y., Machida, T., Katsumoto, M., and Fujinuma, Y.: Variations in atmospheric nitrous oxide observed at Hateruma monitoring station, Chemosphere, 2, 435–443, 2000.

Tohjima, Y., Machida, T., Utiyama, M., Katsumoto, M., and Fujinuma, Y.: Analysis and presentation of in situ atmospheric methane measurements from Cape Ochi-ishi and Hateruma Island, J. Geophys. Res., 107, 4148, doi:10.1029/2001JD001003, 2002.

Yan, X., Cai, Z., Ohara, T., and Akimoto, H.: Methane emission from rice fields in mainland China: Amount and seasonal and spatial distribution, J. Geophys. Res., 108(D16), 4505, doi:10.1029/2002JD003182, 2003.

Yokouchi, Y., Taguchi, S., Saito, T., Tohjima, Y., Tanimoto, H., and Mukai, H.: High frequency measurements of HFCs at a remote site in east Asia and their implications for Chinese emissions, Geophys. Res. Lett., 33, L21814, doi:10.1029/2006GL026403, 2006.

Zeng, J., Tohjima, Y., Fujinuma, Y., Mukai, H., and Katsumoto, M.: A study of trajectory quality using methane measurements from Hateruma Island, Atmos. Environ., 37, 1911–1919, 2003.

Zhang, Q., Streets, D. G., He, K., Wang, Y., Richter, A., Burrows, J. P., Uno, I., Jang, C. J., Chen, D., Yao, Z., and Lei, Y.: NO_x emission trends for China, 1995–2004: The view from the ground and the view from space, J. Geophys. Res., 112, D22306, doi:10.1029/2007JD008684, 2007.

Table 1. Summary of squared correlation coefficients (r^2) of $\sigma_{CO_2}/\sigma_{CH_4}$ and σ_{CO_2} with the national carbon emissions.

	$\sigma_{CO_2}/\sigma_{CH_4}$			σ_{CO_2}	
Country	CDIAC 96-05	EIA 96-05	EIA 96-06	EIA 96-06	EIA 96-06[a]
China	0.91[b]	0.88[b]	0.78[b]	0.44[c]	0.92[b]
Japan	0.84[b]	0.76[b]	0.79[b]	0.31[c]	0.66[d]
Korea	0.40[c]	0.77[b]	0.78[b]	0.21	0.76[b]

[a] The correlation coefficients are calculated except for the σ_{CO_2} values in 1998 and 2003.
[b] Values statistically significant at $p<0.001$
[c] Values statistically significant at $p<0.1$
[d] Values statistically significant at $p<0.01$

ACPD
9, 15725–15746, 2009

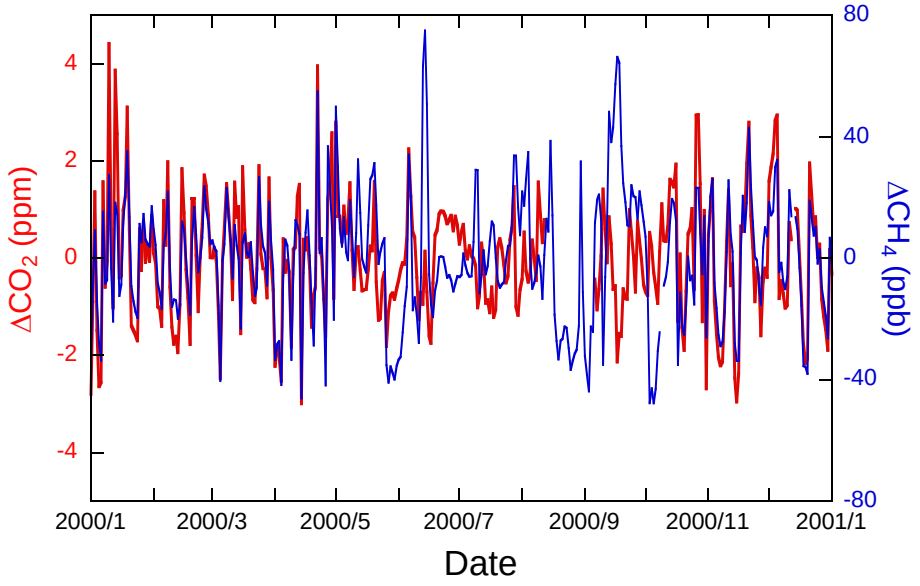

Fig. 1. Time series of the synoptic scale variations (SSVs) in CO_2, (ΔCO_2, red, left axis) and CH_4, (ΔCH_4, blue, right axis) at HAT in 2000. ΔCO_2 and ΔCH_4 are defined as differences between the daily averages and the smooth curve fits to the observed data (see text).

ACPD

9, 15725–15746, 2009

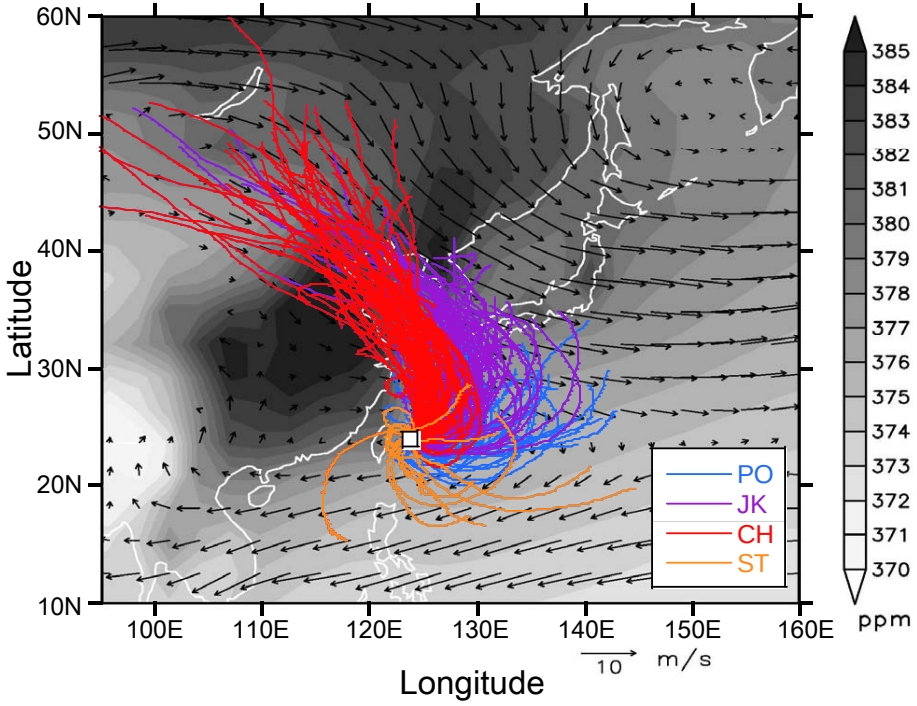

Fig. 2. Three-day backward trajectories for air masses arriving at HAT during the 6 months (January–April and November–December) in 2000. The arrival time of the trajectories is 0600 UTC (1500 JST). The air mass origins are categorized into 4 regions: China (CH, red), Japan and Korea (JK, purple), subtropics (ST, orange), and Pacific Ocean (PO, blue). The distribution of the simulated mean CO_2 concentration at the earth's surface and mean wind vectors (in $m\,s^{-1}$, see legend) at 850 mb height for the 3 months (December–February) are also depicted.

ACPD
9, 15725–15746, 2009

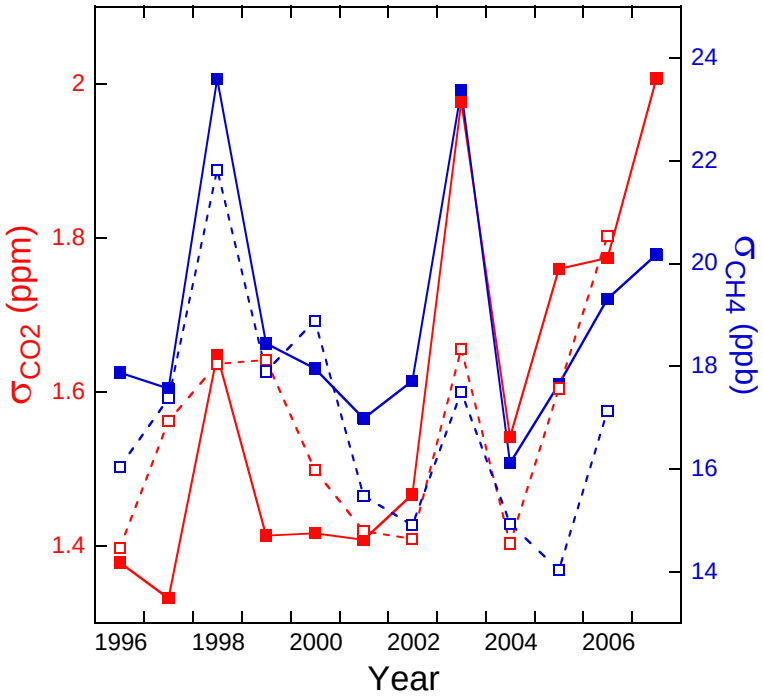

Fig. 3. Temporal changes in the standard deviations of ΔCO_2 (σ_{CO_2}, red) and ΔCH_4 (σ_{CH_4}, blue) based on the data from January to April and from November to December. Closed symbols with solid lines correspond to the observation and open symbols with broken lines correspond to the model simulation.

ACPD

9, 15725–15746, 2009

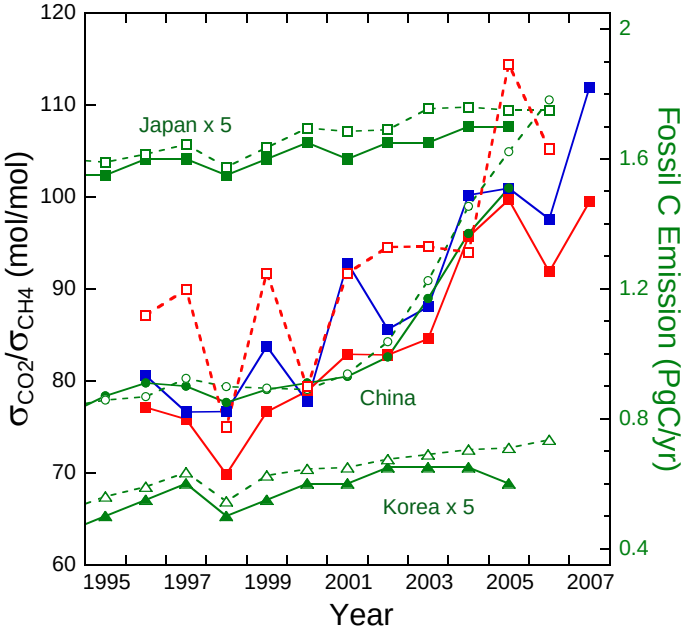

Fig. 4. Temporal changes in the $\sigma_{CO_2}/\sigma_{CH_4}$ ratio for all observation data (closed red squares), selected observation data without the data corresponding to the air masses originating in JK and ST (closed blue squares), and all simulation data (open red squares). Green symbols represent the national carbon emissions form fossil fuel consumption and cement manufacturing for China (circles), Japan (squares), and Korea (triangles). The carbon emissions obtained from CDIAC are depicted as solid symbols and based on EIA as open symbols. The values of the carbon emission from Korea and Japan are multiplied by 5.

ACPD
9, 15725–15746, 2009

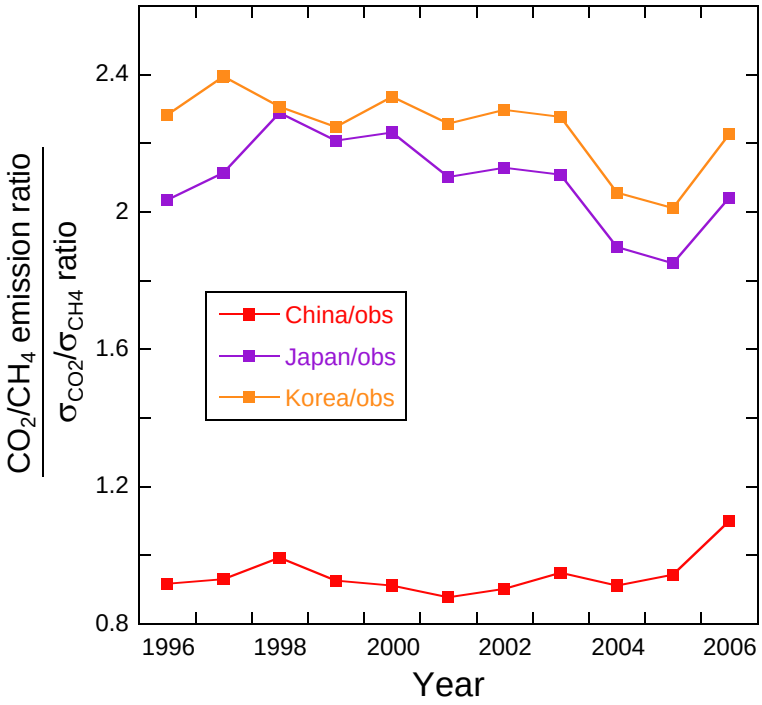

Fig. 5. Interannual variation in the national CO_2/CH_4 emission ratio for China (red), Japan (purple), and Korea (orange) normalized by the $\sigma_{CO_2}/\sigma_{CH_4}$ ratio at HAT. The national CO_2/CH_4 emission ratios are calculated from the November-to-April monthly fluxes used in the model simulation.

ACPD
9, 15725–15746, 2009

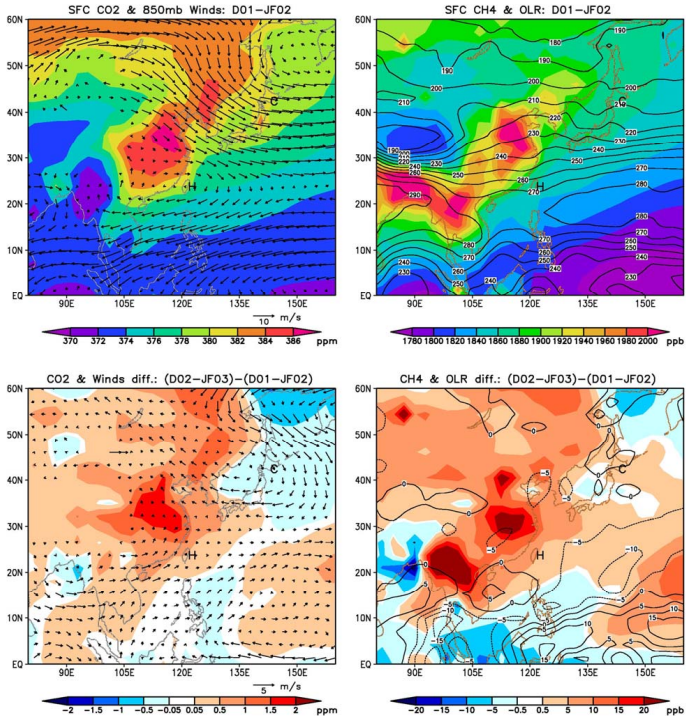

Fig. 6. Examples of 3-monthly (December-February) mean ACTM simulations over the East Asian region. The distributions of CO_2 at surface and wind vectors (in m s^{-1}, see legend) (top left), CH_4 at surface and outgoing longwave radiation (OLR in W m^{-2}; contoured) (top right), interannual differences in CO_2 at surface and wind vectors (bottom left), and interannual differences in CH_4 at surface and OLR (bottom right). The results shown in the top and bottom diagrams correspond to 3-monthly means from December 2001 to February 2002 and the differences between the periods December 2001 to February 2002 and December 2002 to February 2003, respectively.

ACPD
9, 15725–15746, 2009

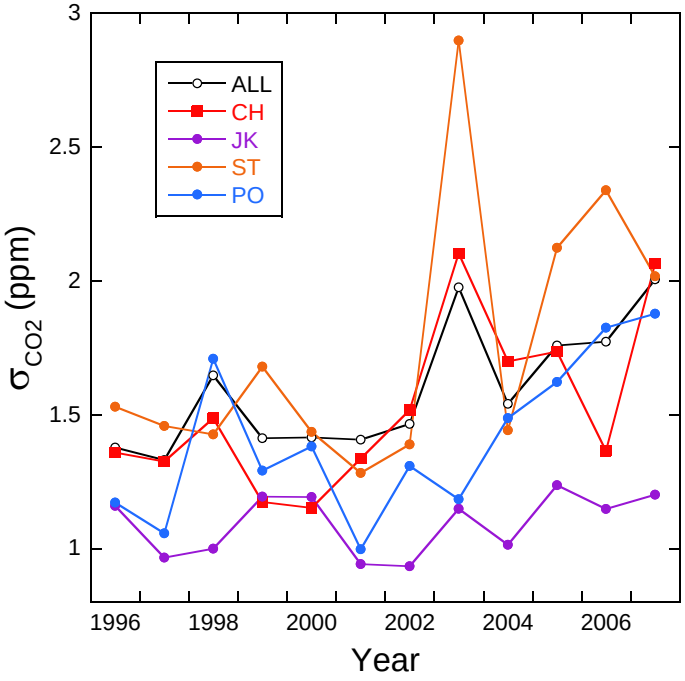

Fig. 7. Temporal changes in the σ_{CO_2} values for the datasets categorized according to the four air mass origins. The σ_{CO_2} values for all data are also depicted as open circle.

ACPD
9, 15725–15746, 2009